HIPPOCAMPUS 17:49–57 (2007)

Characterizing Interneuron and Pyramidal Cells in the Human Medial Temporal Lobe In Vivo Using Extracellular Recordings

Indre V. Viskontas,[1] Arne D. Ekstrom,[2] Charles L. Wilson,[3] and Itzhak Fried[4,5]

ABSTRACT: The goal of this study was to characterize the electrophysiological features of single neurons recorded deep within the medial temporal lobes in humans. Using three physiological criteria to distinguish principal cells and interneurons (firing rate, burst propensity, and action potential waveform) and a large data set of human single neurons (585) from thirteen patients, we show that single neurons in the human MTL separate into two distinct classes comparable to the pyramidal cell and interneuron classes described in animals. We also find that the four different MTL brain regions that we examined (amygdala, hippocampus, entorhinal cortex, and posterior parahippocampal cortex) show unique action potential characteristics, which may in turn relate to the role that neurons from these regions play in behavior. A subset of cells were recorded while patients engaged in both slow-wave (SWS) and rapid-eye movement (REM) sleep and a comparison of the electrophysiological features during these different sleep stages showed that interneurons tended to burst more during SWS compared to REM, while only principal cells in the EC and hippocampus showed a greater propensity for bursting during SWS. Together, our results support the idea that human single neurons have electrophysiologically identifiable cell types, similar to those observed in other mammals, and provide insight into regional and functional differences in spike-wave characteristics relevant to considerations about neural populations in the human brain. © **2006 Wiley-Liss, Inc.**

KEY WORDS: hippocampus; depth electrode; action potential; epilepsy; sleep

INTRODUCTION

Direct neuronal recordings in humans can provide some of the missing pieces of evidence that are needed in order to further our understanding of the neural underpinnings of cognition. While still a rare opportunity, recordings from single neurons in humans in vivo have provided seminal evidence concerning the neuronal correlates of a variety of cognitive functions (Cameron et al., 2001; Kawasaki et al., 2001; Ekstrom et al., 2003; Ojemann et al., 2004; Quiroga et al., 2005; Viskontas et al., 2006). These studies have shown that single neurons respond with both increased firing (Kreiman et al., 2000) or decreased firing (Fried et al., 2002) to a variety of stimuli and during a number of cognitive processes. Little work has been done, however, characterizing the electrophysiological properties of neurons that underlie the responses observed in these studies.

In the rat hippocampus, firing rate, action potential duration, and bursting propensity have been shown to effectively separate cells into classes of interneurons and pyramidal cells (Ranck, 1973; Csicsvari et al., 1999); this classification has been further validated by in vivo intracellular labeling as well as via simultaneous intra and extracellular recordings from the same neuron types (Henze et al., 2000; Klausberger et al., 2003). To date, no such classification has been attempted in the human hippocampus by using in vivo extracellular recordings. Using these criteria, we explored the physiological characteristics of 585 single neurons recorded from the medial temporal lobes in humans during a variety of different recordings collected in our lab. We were also interested in observing any regional differences in these cell features throughout the medial temporal lobe. To this end, we included cells from four regions: the amygdala (mainly the basal nucleus), hippocampus proper (mainly CA fields), entorhinal cortex, and posterior parahippocampal cortex. Finally, because previous studies have shown shifts in firing patterns with different sleep states (Fox and Ranck, 1981), we wondered whether the sleep stage of the patient could result in differences in the cell spiking features. In fact, previous work has shown that single neurons within the human MTL show a greater propensity for bursting than during slow-wave sleep (SWS) than during rapid-eye movement (REM) sleep (Staba et al., 2002a). To find out if this burst propensity difference was specific to a particular cell type, we compared features for the same set of cells during REM and SWS.

METHODS

Patients

Participants were patients with pharmacologically-resistant epilepsy for whom extensive noninvasive evaluation failed to yield a single epileptogenic zone. To obtain localizing information for potential curative resection, patients were stereotactically implanted with 6–14 electrodes from a lateral orthogonal approach

[1] **Department of Psychology, University of California, Los Angeles, California;** [2] **Ahmanson-Lovelace Brain Mapping Center, University of California, Los Angeles, California;** [3] **Department of Neurobiology, David Geffen School of Medicine, University of California, Los Angeles, California;** [4] **Division of Neurosurgery, David Geffen School of Medicine and Semel Institute for Neurosciences and Human Behavior, University of California, Los Angeles, California;** [5] **Functional Neurosurgery Unit, Tel Aviv Medical Center and Sackler School of Medicine, Tel Aviv University, Israel**

Grant sponsor: National Institute of Neurological Disorders and Stroke (National Institutes of Health); Grant numbers: NS 33221, NS33310, NS 02808, F32 NS50067-01; Grant sponsor: Natural Science and Engineering Research Council of Canada (IVV).

*Correspondence to: Dr. Itzhak Fried; Division of Neurosurgery, David Geffen School of Medicine at University of California, 740 Westwood Plaza, Los Angeles, CA 90095-7039. E-mail: ifried@mednet.ucla.edu

Accepted for publication 21 September 2006
DOI 10.1002/hipo.20241
Published online 1 December 2006 in Wiley InterScience (www.interscience.wiley.com).

and aimed at targets selected using clinical criteria (surgeries were performed by I.F.). Following implantation patients were monitored for spontaneous seizures on the ward. All patients provided informed consent and every session conformed to the guidelines of the Medical Institutional Review Board at UCLA. Based on depth EEG recordings and other clinical criteria, epileptogenic zones were localized by neurologists and neurosurgeons for possible resection planning. These areas were determined (in part) by examining EEG recordings accompanying seizures and determining from which depth contacts epileptiform activity spread (Rosenow and Luders, 2001). In general, only a small number of the total recording electrodes included contacts in regions where seizures were thought to originate. All patients had bilaterally implanted depth electrodes in multiple sites in order to contrast rival hypotheses about seizure location. For the purposes of the present study, epileptogenic zones were defined as the temporal lobes in which spontaneous seizure onsets occurred.

Recordings

At the tips of each electrode was a set of nine 40-μm platinum–iridium microwires: the 9th microwire served as a reference, while the other 8 microwires provided possible cellular signals. Anatomical locations of electrodes were verified via postplacement magnetic resonance imaging (MRI) scans and images created by fusing CT scans taken while electrodes were implanted with high resolution MRI scans taken immediately before implantation (Fried et al., 1999).

Signals from each microwire were amplified (gain = 10,000), digitally sampled at 27.8 kHz, and bandpass filtered between 1 and 6 kHz (Neuralynx, Tucson, AZ). Using the spike separation algorithm *wave_clus* (Quiroga et al., 2004), we isolated single unit activity during microwire recordings. Single units were defined as waveforms with clear refractory periods, were of high amplitude (>25 mV), and when displayed as an interspike interval (ISI) histogram, had less than 1% of spikes occurring at less than 3 ms from one another; waveforms that appeared to be contaminated by more than one cell were labeled "multi-units" and were excluded. As an additional check for noise, we plotted the power spectral density (PSD) by using the times when spikes occurred for that unit; putative cell activity showing significant amounts of 60 Hz power-line activity were excluded from the analysis.

Characterizing Cell Features Using Extracellular Recordings

For each single unit we isolated, several parameters were extracted from the spike waveform to characterize its shape and timing. We were primarily interested in three parameters described by Csicsvari et al. (1999) that were useful in distinguishing interneurons from principal cells in the hippocampus with extracellular recordings: firing rate, burst propensity, and action potential duration. We also included an analysis using firing rate, burst propensity, and the relative amplitudes of the spike and the wave that follows it, since amplitude is related to duration and may provide additional clustering information.

Measure of Firing Rate

Firing rate was calculated for each unit by measuring the total number of spikes divided by the total duration of the recording session.

Measures of Action Potential Duration and Amplitude

To evaluate action potential waveforms, we used different measures of action potential duration and one measure of action potential amplitude. Using linear interpolation, we estimated the slope of the rise of waveform and the slope of the fall of the waveform (return to baseline and opposite polarity) (see Fig. 1 and Csicsvari et al., 1999; Henze et al., 2000).

The rise-time (t_1) is defined to be the time at which the action potential first begins to rise and show a positive slope; a_1 is the voltage of the waveform at t_1. Peak-time (t_2) is the time at which the action potential reaches the highest voltage (a_2, voltage of waveform at t_2) and when the cell first begins to return to baseline. The fall-time (t_3) is the time at which the waveform first returns to baseline and reaches a voltage equal to that at which it first began to rise (a_3, voltage of waveform at t_3, $a_1 = a_3$). The valley-time (t_4) is defined to be the time of maximal polarity in the opposite direction after the initial spike (a_4, voltage of waveform at t_4). Finally, the return-time (t_5) is the time at which the waveform returns to baseline (a_5, voltage of waveform at t_5).

Our first measure, which we call overall waveform duration, was the time at which the action potential returned to its resting baseline value minus the rise-time ($t_5 - t_1$). A second measure, called spike slope ratio, was defined as the ratio of the slope of the rise of the action potential divided by the slope of the fall of

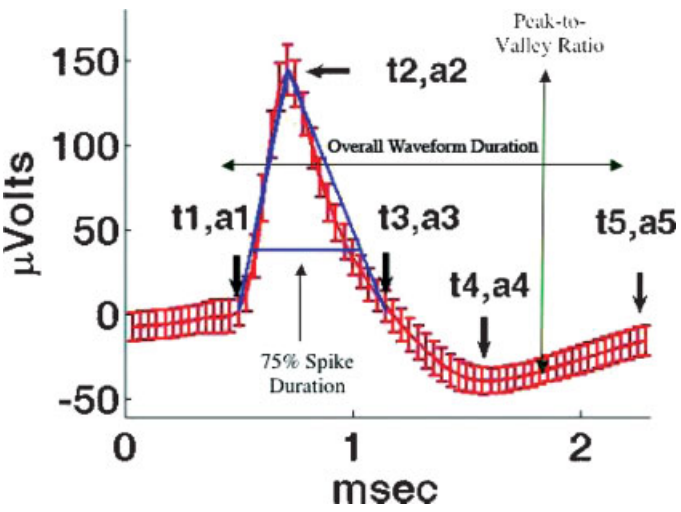

FIGURE 1. Measures of action potential duration and amplitude. Mean spike waveform displaying measures of action potential duration and amplitude: overall waveform duration, 75% spike duration, spike–slope ratio, and peak-to-valley ratio. The polarity of the waveforms is negative, but for illustration purposes, we have inverted the polarity of the waveforms (negative = up). [Color figure can be viewed in the online issue, which is available at www.interscience.wiley.com.]

the action potential (spike slope ratio = $((a_2 - a_1)/(t_2 - t_1))/((a_3 - a_2)/(t_3 - t_2))$). For a third measure, we calculated the interval between 25% of the rise-time and 75% of the fall-time (75% spike duration = $((t_2 - t_1)25 + t_1) - ((t_3 - t_2)75 + t_2)$. Finally the ratio of the height of the amplitude of the action potential divided by the lowest amplitude of the action potential during the refractory period was defined as the peak-to-valley ratio (peak-to-valley ratio = a_2/a_4).

Measures of Burst Propensity

We extracted two parameters from the ISIs to calculate two estimates of bursting propensity. The burst value was defined as the time of the mean (x_1) of the autocorrelogram for a given cell; that is, x_1 is the point in time at which the mean of the autocorrelogram occurred. The autocorrelogram was computed by correlating the spike train with itself using 2 ms bins and calculating the total number of spikes that occurred in that bin and at different time lags. The autocorrelogram thus provides a measure of the degree of repetitions in spike bursts for a spike train. Cells that display more bursting will show a narrower autocorrelogram, and therefore should show mean values at shorter time points, leading to a lower burst value. A second measure, the burst interspike interval (ISI) ratio, was calculated by dividing the total number of spikes that occurred at less than 10 ms of each other by the total number of spikes that occurred at greater than or equal to 10 ms of each other. Thus, a cell with a high burst ISI ratio had a greater proportion of ISI occurring at less than 10 ms than at the slower ISIs, and therefore showed greater bursting propensity.

Firing in the Theta (4–8 Hz) Range

Previous findings from the animal literature (Csicvari et al., 1999) indicate a role for interneurons in theta-modulation. To investigate whether our putative interneurons were more likely than putative pyramidal cells to show firing in the theta-band, we measured the Fourier transformed PSD of cellular firing in the theta band for humans (4–8 Hz) (Neidermeyer, 1999). We then normalized this measure by the mean power (Fourier-transformed spectral density) for each cell.

Recordings

Unit activity was recorded while the patient was engaged in one of three different behavioral tasks or during SWS. During the behavioral sessions, the patient was engaged in cognitive tasks involving attending to stimuli on a laptop computer and making appropriate responses via key presses. Data from three cognitive tasks are included here: a recognition memory task, a virtual navigation task followed by a memory test for items encountered during navigation, and a task involving the observation and imitation of hand movements. There were no differences in waveform characteristics from the different behavioral tasks. Therefore, different tasks were simply treated as unique sessions for each patient. All behavioral testing sessions occurred between the hours of 9 AM and 9 PM. Recordings during sleep took place between 10 PM and 7 AM.

Unit Activity During REM and SWS

For the purposes of this analysis, we analyzed one continuous 30–50 min REM/SWS session per night, in order to reduce the possibility of any change in action potential amplitude or shape. We counterbalanced the order of REM and SWS episodes across patients so that for all sleep sessions analyzed each stage was equally likely to occur first in the recording session. We performed this counterbalancing procedure to ensure that we did not find differences between stages that could be accounted for simply by the passage of time. The entire sleep session, including both REM and SWS, was used during the detection of single-units. Therefore, the features pertaining to the same cells could be compared during REM and SWS.

Sleep Stages

Sleep stages were scored using the method of Rechtschaffen and Kales (1968). Two Electro-oculogram (EOG) leads were placed on the outer canthus of each eye, two on each side of the mentalis muscle of the chin and one on each ear lobe for EOG and Electromyography (EMG) recording. Cortical leads were recorded at C3 and C4. Sleep records were scored using a Telefactor work station in 30 s review segments, and hypnogram epochs of at least 10 min were used in which either REM sleep or SWS were identified. Cortical slow waves accompanied by low voltage EMG and absence of phasic EOG were scored as SWS (stages 3 and 4). Cortical desynchronization accompanied by low voltage EMG and phasic EOG were scored as REM sleep.

Clustering According to Cell Features

To classify cells as putative interneurons or principal cells, all single units from the four MTL regions were used in a K-means cluster analysis (MacQueen, 1967) using three parameters: firing rate, burst ISI ratio, and a measure of action potential duration, 75% spike duration. We ran a second cluster analysis using firing

TABLE 1.

Cell Features for Putative Interneuron and Pyramidal Cell Clusters

	Cluster 1: interneurons		Cluster 2: principal cells	
Cell feature	Mean	S.D.	Mean	S.D.
A: firing rate (Hz)	10.77	±9.39	1.99	±1.97
B: firing rate (Hz)	9.79	±10.51	2.18	±2.42
A: burst ISI (ratio)	0.34	±0.28	0.05	±0.05
B: burst ISI (ratio)	0.42	±0.27	0.05	±0.05
A: peak-to-valley (ratio)	4.97	±1.12	4.33	±1.00
B: 75% spike duration (ms)	0.643	±0.23	0.584	±0.20

Values labeled A denote clusters classified using peak-to-valley ratio (Cluster 1, $n = 41$; Cluster 2, $n = 544$) whereas those labeled B denote clusters classified using 75% spike duration (Cluster 1, $n = 33$; Cluster 2, $n = 552$).

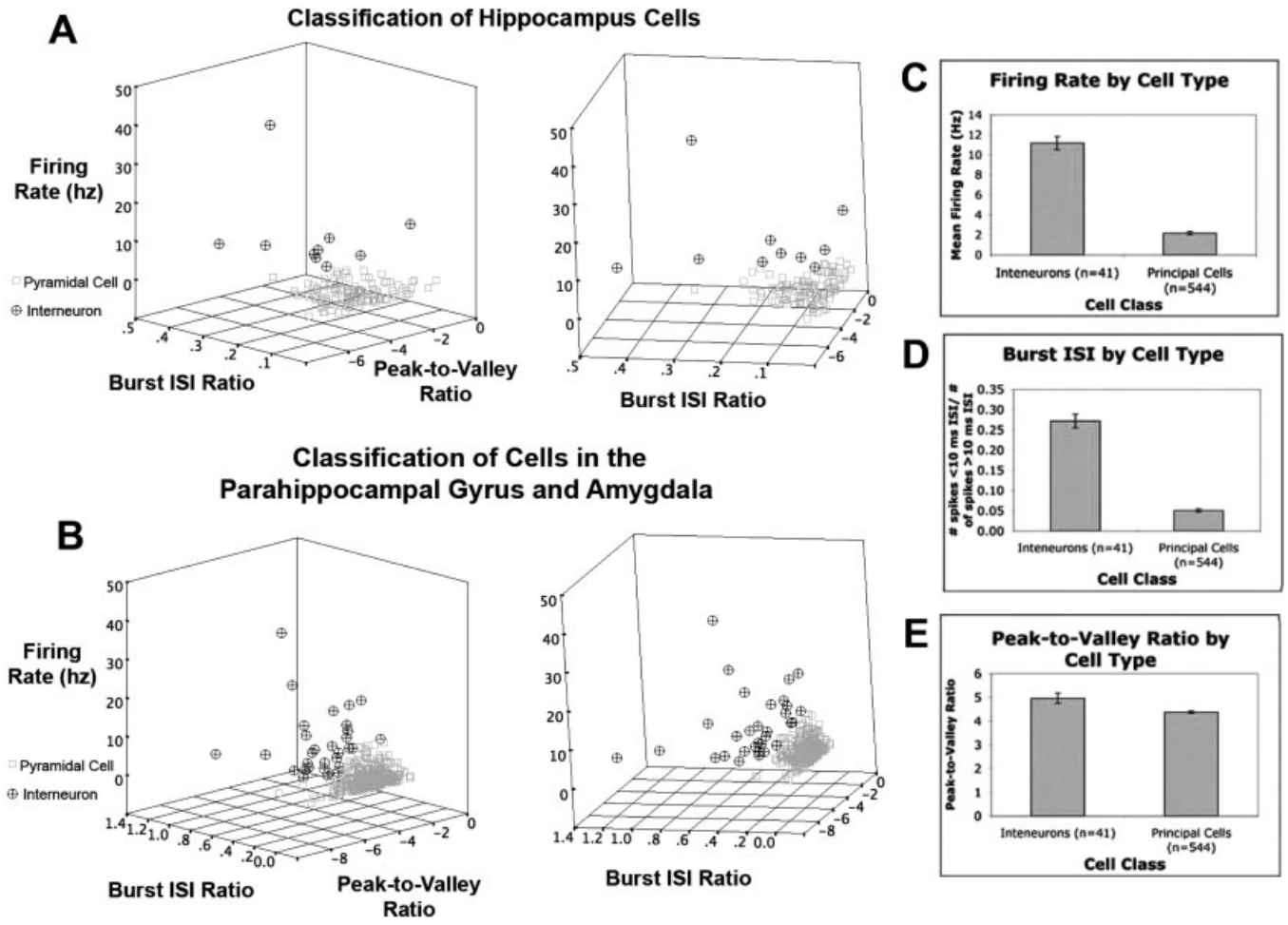

FIGURE 2. Clustering by cell type. Using a K-means cluster analysis, two distinct clusters of cells are visible in our single neuron population. (A) represents clustering using firing rate, burst ISI ratio, and peak-to-valley ratio in the hippocampus, in two views while (B) shows clustering in regions outside of the hippocampus, also in two views. Cluster 1 corresponds to the putative interneuron sample, while Cluster 2 corresponds to the putative principal cell cluster, as defined in the K-means cluster analysis. Note the different scales in burst ISI ratio in (A) and (B), since two interneurons outside of the hippocampus show burst ISI ratios of >1. (C–E) show that putative interneurons in all regions had higher firing rates, more bursting, and larger action potential amplitudes than the putative pyramidal cells. Error bars reflect the standard error of the mean.

rate, burst ISI ratio, and our measure of the relative amplitudes of the spike and the wave that follows it, the peak-to-valley ratio. We chose the K-means cluster analysis in part because we could specify the number of clusters (2), and the algorithm minimizes variance within a cluster by minimizing the Euclidean distance between each point and the centroid, thereby maximizing the variability between clusters. Before running the analysis, we standardized all of the variables and used the z-scores in the analysis.

RESULTS

We recorded the activity of 585 single neurons from 13 patients: nine participated in the behavioral recording sessions, seven participated in the recordings during sleep, and three patients participated in both behavior and sleep sessions. Because we included multiple recording sessions from several of the patients, we wanted to ensure that we were not recording activity in the same cells more than once. To this end, we examined the correlations of each of our parameters between the two recording sessions occurring closest to each other in time in the same patients. It should be noted, however, that sessions were separated by at least 48 h. This analysis of 138 pairs of single units showed that there were no significant correlations (Spearman's Rho) between any of the measures of firing rate, action potential duration, relative action potential amplitudes, or burst propensity, from one session to another (r values ranged from –0.120 to 0.102; all $P < 0.1$). Therefore, in the remainder of our analyses, we considered channels recorded over multiple sessions in the same patients separately.

K-means Cluster Analysis

Using z-scores of the three parameters, both K-means cluster analyses identified two final cluster centers that were significantly different on all three parameters ($P < 0.001$). Table 1 shows the

mean values for each parameter for the two resulting clusters for both of these analyses. The results of both analyses showed very similar clustering, with only the nine fewer cells classified as putative interneurons using the measure of action potential duration, and one extra cell was classified as a pyramidal cell.

To eliminate skew and to ensure homogeneity of variance (using Levene's test of homogeneity) between the clusters, we transformed the raw data using an inverse transformation for firing rate and a log transformation for burst ISI ratio. For clustering using the peak-to-valley ratio, a one-way analysis of variance (ANOVA) revealed that the two clusters showed significantly different firing rates ($F(1,584) = 5.837$, $P < 0.016$), burst ISI ratio ($F(1,584) = 46.06$, $P < 0.001$), and peak-to-valley ratios ($F(1,584) = 15.14$, $P < 0.001$). Similar results were seen in the clusters generated using the 75% spike duration, except that the difference between the clusters with respect to spike duration was only marginally significant: firing rate ($F(1,585 = 4) = 38.55$, $P < 0.001$), burst ISI ratio ($F(1,584) = 57.67$, $P < 0.001$), and 75% spike duration ($F(1,584) = 2.76$, $P < 0.097$). Therefore for the remainder of the analyses, we used the clustering generated by the peak-to-valley ratio, since this measure yielded a significant difference between clusters. Figure 2 shows the clustering with respect to cell features and Figure 3 shows two representative autocorrelograms.

Firing in the Theta-Band

We compared normalized theta-band power from putative interneurons and a representative pseudorandomly-selected sample of similar size from the putative pyramidal cells using an independent samples *T*-test. We found that putative interneurons showed a greater propensity for theta-band firing than putative pyramidal cells ($T(79) = 2.63$, $P < 0.01$). Given the small size of our interneuron sample, we were unable to investigate regional differences. These data are shown in Figure 4.

Epileptogenic Zones

To investigate whether cell features differed in regions suspected to be within or outside epileptogenic zones, we ran an ANOVA using epileptogenic zones and cell types (interneurons vs. principal cells) as between-subject factors for each cell feature. We found that there was no significant main effect of epileptogenic zone on any of these measures, nor were there any significant interactions with cell-type. Since there was no effect of epileptogenicity on cell features, we included all cells recorded both inside and outside of epileptogenic zones in the analyses reported in the present study.

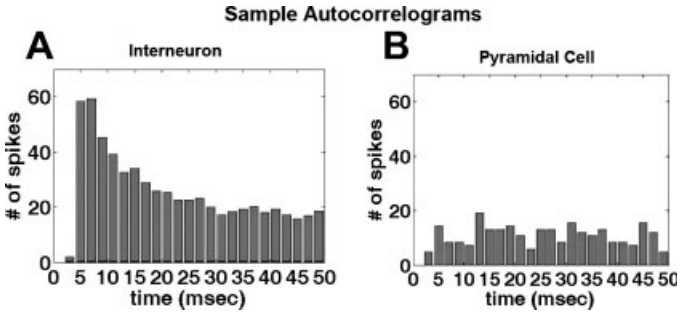

FIGURE 3. Representative autocorrelograms for (A) a putative interneuron and (B) a putative pyramidal cell.

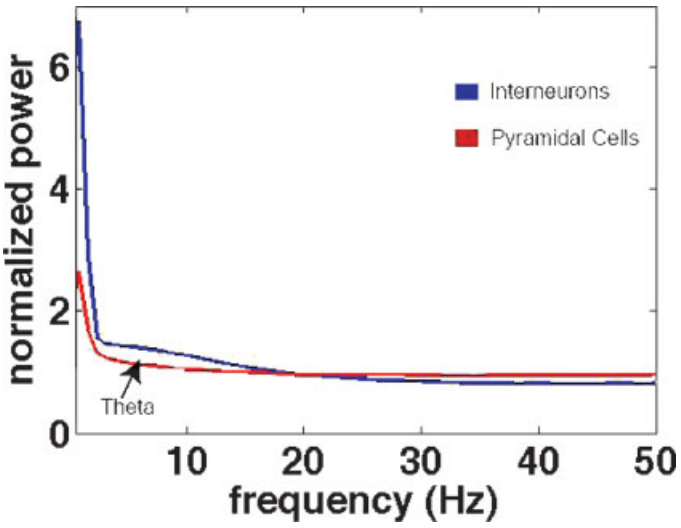

FIGURE 4. Mean PSD functions for interneurons (blue) and pyramidal cells (red). Note that interneurons show more power in the theta-band (4–8 Hz) than pyramidal cells. [Color figure can be viewed in the online issue, which is available at www.interscience.wiley.com.]

Regional Differences in Cell Features for Classified Single-Units

Using the results of the K-means cluster analysis on the single-units, we investigated the differences in cell features for the two cell types (putative interneurons and putative principal cells) in the four different MTL regions (amygdala, entorhinal cortex, hippocampus, and parahippocampal gyrus). We performed a 2 (interneurons vs. principal cells) × 4 (amygdala, entorhinal cortex, hippocampus, and parahippocampal gyrus) ANOVA with dependent measures being each of the parameters describing spike features: firing rate, burst value, burst ISI ratio, spike slope ratio, overall waveform duration, 75% spike duration, and the peak-to-valley ratio. Table 2 shows the numbers of cells in each cluster for each MTL region.

TABLE 2.

Regional Distributions of Cell Types

Region	Cluster 1 interneurons	Cluster 2 principal cells
Amygdala ($n = 196$)	17	179
Entorhinal cortex ($n = 205$)	9	196
Hippocampus ($n = 119$)	10	109
Parahippocampal gyrus ($n = 65$)	5	60

TABLE 3.

Regional Differences in Cell Features

Region	Firing rate (Hz)	Spike slope ratio	75% spike duration (ms)	Overall waveform duration (ms)	Peak-to-valley ratio
Amygdala ($n = 196$)	5.20 ± 0.38	−2.03 ± 0.05	0.59 ± 0.02	0.88 ± 0.04	4.59 ± 0.12
Entorhinal cortex ($n = 182$)	7.29 ± 0.80	−2.20 ± 0.05	0.58 ± 0.05	1.06 ± 0.09	4.65 ± 0.26
Hippocampus ($n = 119$)	8.4 ± 0.53	−1.89 ± 0.06	0.48 ± 0.03	0.71 ± 0.06	5.22 ± 0.17
PPHC ($n = 65$)	5.79 ± 0.86	−2.06 ± 0.03	0.57 ± 0.06	0.90 ± 0.09	4.23 ± 0.28

Values given are mean ± SE.

Interneuron and principal cell clusters showed significant differences only on those parameters that were used in the initial clustering (firing rate, burst ISI ratio, and peak-to-valley ratio). Of note, we did not find differences between the clusters in burst value (putative interneuron mean = 24.56 ± 12.14, putative pyramidal cell mean = 24.91 ± 14.21). There were, however, significant interactions between region and cell cluster for firing rate ($F(3,585) = 2.70$, $P < 0.045$), spike slope ratio ($F(3,585) = 4.75$, $P < 0.003$), overall waveform duration ($F(3,585) = 3.15$, $P < 0.025$), and 75% spike duration ($F(3,585) = 2.82$, $P < 0.038$). These results are shown in Table 3. Post hoc tests revealed that for firing rate there was a significant difference between interneurons and principal cells in all of the four regions (hippocampus, $P < 0.001$; amygdala, $P < 0.001$; entorhinal cortex, $P < 0.001$; and posterior parahippocampal gyurs, $P < 0.025$). For each measure of spike duration, only the hippocampus showed significant differences between interneurons and pyramidal cells (for spike slope ratio, $P < 0.002$; for overall waveform duration, $P < 0.006$; for 75% spike duration, $P < 0.032$) with interneurons showing shorter spike durations than pyramidal cells. These results are shown in Figure 5.

Differences in Cell Features During REM and SWS

For a subset of our cells, we had information about their cell features during two stages of sleep: REM and SWS (stages 3 and 4). In this subset, our K-means cluster classification rendered 13 putative interneurons and 276 putative principal cells across our four MTL regions. Eight of these 13 putative interneurons were located in the amygdala, preventing a meaningful analysis of the effects of sleep stage on interneurons separately for each region. Therefore, we performed paired *t*-tests for each cell feature on the interneurons. To eliminate skew, we used log transformations of firing rate and burst ISI ratio. We found a significant difference in burst ISI ratio for REM and SWS sleep in our interneuron population ($t(12) = 3.63$, $P < 0.003$), with a higher burst ISI ratio and therefore more bursting during SWS. Previous research has also shown that cells in the EC and hippocampus show greater bursting during SWS (Staba et al., 2002a). Therefore, we performed paired *t*-tests on burst ISI ratio for REM and SWS in pyramidal cells recorded in the EC and hippocampus. We did in fact see greater bursting in these regions during SWS ($t(141) = 2.10$, $P < 0.05$), but not in the amygdala and posterior parahippocampal cortex ($t < 1$). There were no other significant differences in firing rate or any of the spike duration measures for either principal cells or interneurons.

DISCUSSION

Cell Classification

Our clustering algorithm successfully classified our single-units into two distinguishable populations: a large population of putative pyramidal cells and a second much smaller population of putative interneurons. It is important to note, however, that we cannot definitively determine cell types in these patients since in vivo intracellular recordings are of course not possible for ethical reasons. In our classification, the relative sizes of these putative interneuron and principal cell populations correspond to the actual proportions of principal cells and interneurons in the medial temporal lobe as measured in rodents: the vast majority of cells are principal or pyramidal cells while less than 10% of cells are interneurons (Freund and Buzsaki, 1996). In our sample of 585 single cells, 41 (7%) were classified as putative interneurons. In fact, in a similar study designed to classify interneurons and principal cells in the neocortex, Bartho et al. (2004) found exactly 7% of cells were considered putative interneurons. Furthermore, our putative interneurons showed much higher firing rates than the pyramidal cells (10.77 ± 1.47 Hz (mean ± SE) and 1.99 ± 0.08 Hz, respectively), and these firing rates were close to rates observed in the rat (interneurons, 14.1 ± 1.43 Hz; pyramidal cells, 1.4 ± 0.01 Hz; Csicsvari et al., 1999). These findings of electrophysiologically identifiable neuronal groups in the human hippocampus provide important validation for extending studies of interneurons in rodents and lower mammals to the human brain. Our data further suggest that computational models involving interneurons and principal cells based on the rat brain (e.g., Colom and Bland, 1987; Bland et al., 2002; Nitz and McNaughton, 2004) likely will have validity for the human brain as well. Our results also show that cognitive electrophysiology studies are justified in separating cells into distinct populations (e.g., Ekstrom et al., 2003); our analysis methods therefore provide a way to do this based on firing rate, bursting propensity, and waveform shape. In the absence of intracellular recordings or slice physiology, our method provides valuable information as to the nature of the cells from which recordings are taken.

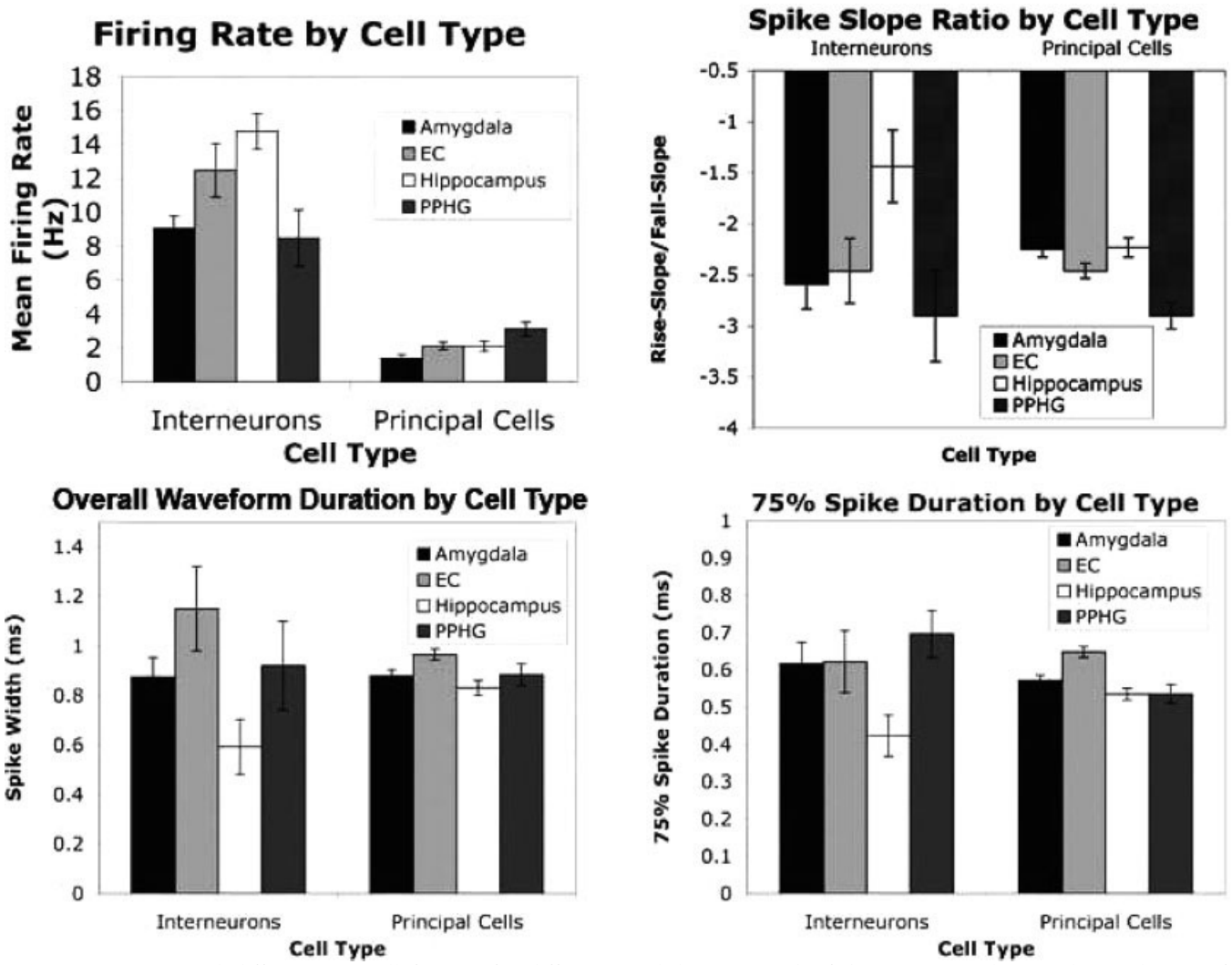

FIGURE 5. Regional differences in cell features for different cell types. All four regions showed differences in mean firing rates between interneurons and principal cells. Only the hippocampus, however, showed differences in the three measures of action potential duration. Each of these measures shows a shorter duration for interneurons than for pyramidal cells. Error bars reflect the standard error of the mean.

Epileptogenic Zones

Of note, we did not find any differences in cell features for single cells in or outside of the epileptogenic zones. Therefore, we included units recorded from regions both inside and outside of epileptogenic zones in analyses of single neuron activity. These data also suggest that even in epileptogenic areas of the human brain, action potentials from single neurons, particularly those engaged during sleep and behavior, are not altered significantly as measured in the present study.

Regional Differences in Cell Features

Strikingly, we found that only in the hippocampus, putative interneurons showed shorter spike durations than putative pyramidal cells. In fact, Figure 6 shows that the median waveform in our interneuron sample is slightly narrower while the spike amplitude is greater; an observation that is consistent with the differences seen between interneurons and pyramidal cells in the hippocampus in rodents (Csicsvari et al., 1999). Consistent with the animal literature, interneurons showed shorter action potential durations than pyramidal cells in the hippocampus (Csicsvari et al., 1999) but not in any other MTL region. This regional difference is responsible for the small effect of spike duration in our classification: when all the regions are considered, the effect found in the hippocampus is washed out by the null effect in the surrounding regions. Furthermore, shorter action potential durations have been found in interneurons during both intracellular (Buhl et al., 1996) and extracellular (Henze et al., 2000) recordings.

Our analysis of regional differences in cell features among our clustered single-units also revealed significant differences between putative pyramidal cells in the hippocampus/entorhinal cortex and those found in the amygdala and more posterior in the parahippocampal gyrus. Although pyramidal cells in the hippocampus and entorhinal cortex shared fairly similar waveform shapes, the cells in the other regions showed distinctly smaller action potential

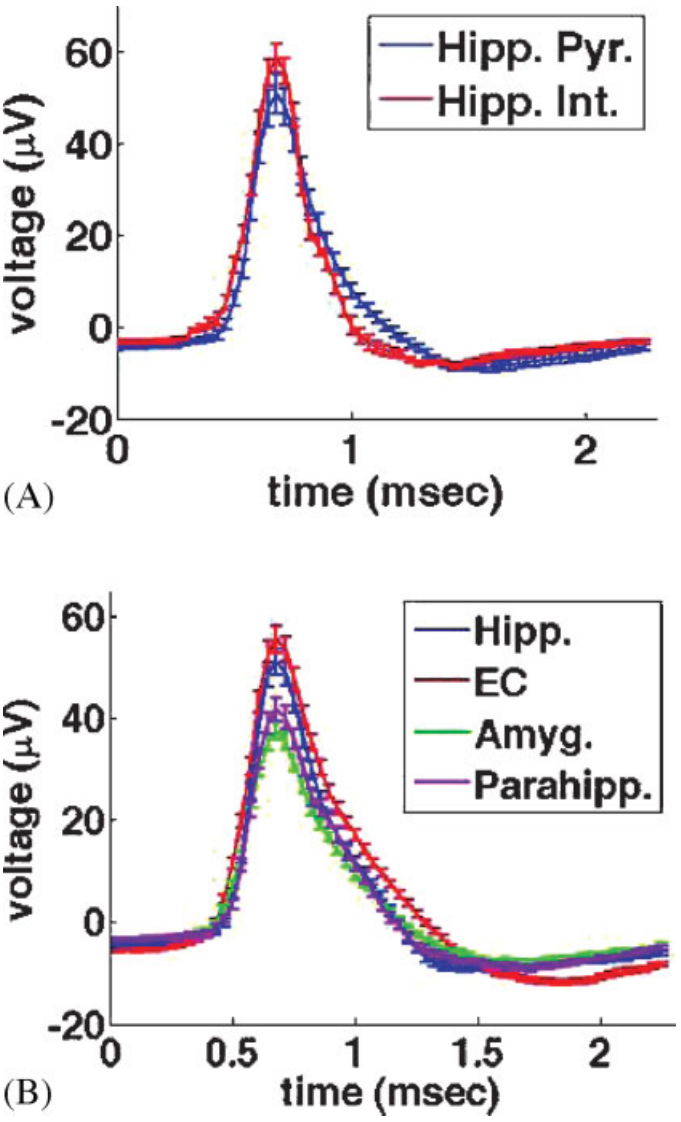

FIGURE 6. Median waveforms. (A) shows the difference in the median waveform shape for interneurons and pyramidal cells in the hippocampus. Hippocampal interneurons show more narrow action potentials. (B) shows the median waveforms for pyramidal cells in each of the four MTL regions. Error bars reflect the standard error of the mean. [Color figure can be viewed in the online issue, which is available at www.interscience.wiley.com.]

amplitudes. The entorhinal cortex has long been considered to be the major input provider to the hippocampus, and for this reason, it is not surprising that the pyramidal cells in these highly interconnected regions should show similar firing properties. Entorhinal cortex pyramidal cells had longer spike durations and took more time to return to baseline, while hippocampal pyramidal cells showed narrower waveforms. These results point to the importance of using several measures of cell features, as each measure provides unique information about the action potential. Caution must be used when interpreting these results; however, as anatomical differences between regions may account for differences in electrophysiological properties. In addition, high-pass filtering may have affected our ability to observe subtle differences in waveform shape.

REM Versus SWS

SWS is characterized by the presence of sharp waves (discrete cooperative neuronal bursts) that are thought to affect synaptic plasticity and therefore may be critical for memory consolidation in the hippocampus (Buzsaki, 1998). Furthermore, it is likely that sharp waves are initiated by bursting activity in interneurons (Ylinen et al., 1995). Our finding that interneurons show a greater propensity for bursting during SWS than during REM is consistent with the idea that interneuron bursting is involved in the generation of sharp waves. Thus, the increased bursting we observed in our interneuron population during SWS suggests that some of the same mechanisms underlying sharp-wave generation, and possibly memory consolidation, could be at work in the human brain as it is in other mammals. We also found that pyramidal cells show greater bursting during SWS than during REM in both the entorhinal cortex and hippocampus. This finding is consistent with previous work in both humans (Staba et al., 2002a,b) and rodents (Buzsaki, 1986) and gives further evidence to the hypothesis that memory consolidation during SWS involves hippocampal–neocortical interaction during sharp-wave periods.

CONCLUSION

The main finding of our study is that our classification method yielded two distinct, electrophysiologically identifiable cell types in the human medial temporal lobe, which segregate on the basis of firing rate, burst propensity, and action potential amplitude. In addition, we found regional differences in the medial temporal lobe with respect to waveform shapes. Hippocampal and entorhinal neurons tended to show greater amplitude waveforms overall. Interneurons in the hippocampus showed shorter spike durations than pyramidal cells in this region, a finding that is consistent with the rodent literature. Finally, putative interneurons, once classified as such using the three criteria described earlier, showed more bursting during SWS than during REM sleep.

Acknowledgments

We thank the patients for participating in our study. We also thank Kristen Upchurch, Tony Fields, Emily Ho, Jennifer Ogren, and Eve Isham for technical assistance related to this work.

REFERENCES

Bartho P, Hirase H, Monconduit L, Zugaro M, Harris KD, Buzsaki G. 2004. Characterization of neocortical principal cells and interneurons by network interactions and extracellular features. J Neurophysiol 92: 600–608.

Bland BH, Konopacki J, Dyck R. 2002. Relationship between membrane potential oscillations and rhythmic discharges in identified hippocampal theta-related cells. J Neurophysiol 88:3046–3066.

Buhl EH, Szilagyi T, Halasy K, Somogyi P. 1996. Physiological properties of anatomically identified basket and bistratifed cells in the CA1 area of the rat hippocampus in vitro. Hippocampus 6:294–305.

Buzsaki G. 1986. Hippocampal sharp waves: Their origin and significance. Brain Res 398:242–252.

Buzsaki G. 1998. Memory consolidation during sleep: A neurophysiological perspective. J Sleep Res 7:17–23.

Cameron KA, Yashar S, Wilson CL, Fried I. 2001. Human hippocampal neurons predict how well word pairs will be remembered. Neuron 30:289–298.

Colom LV, Bland BH. 1987. State-dependent spike train dynamics of hippocampal formation neurons: Evidence for theta-on and theta-off cells. Brain Res 422:277–286.

Csicsvari J, Hirase H, Czurko A, Mamiya A, Buzsaki G. 1999. Oscillatory coupling of hippocampal pyramidal cells and interneurons in the behaving rat. J Neurosci 19:274–287.

Ekstrom AD, Kahana MJ, Caplan JB, Fields TA, Isham EA, Newman EL, Fried I. 2003. Cellular networks underlying human spatial navigation. Nature 425:184–188.

Fox SE, Ranck JB Jr. 1981. Electrophysiological characteristics of hippocampal complex-spike cells and theta cells. Exp Brain Res 41:399–410.

Freund TF, Buzsaki G. 1996. Interneurons of the hippocampus. Hippocampus 6:347–470.

Fried I, Wilson CL, Maidment NT, Engel J Jr, Behnke E, Fields TA, MacDonald KA, Morrow JW, Ackerson L. 1999. Cerebral microdialysis combined with single-neuron and electroencephalographic recording in neurosurgical patients. J Neurosurg 91:697–705.

Fried I, Cameron KA, Yashar S, Fong R, Morrow JW. 2002. Inhibitory and excitatory responses of single neurons in the human medial temporal lobe during recognition of faces and objects. Cereb Cortex 12:575–584.

Henze DA, Borhegyi Z, Csicsvari J, Mamiya A, Harris KD, Buzsaki G. 2000. Intracellular features predicted by extracellular recordings in the hippocampus in vivo. J Neurophysiol 84:390–400.

Kawasaki H, Kaufman O, Damasio H, Damasio AR, Granner M, Bakken H, Hori T, Howard MA III, Adolphs R. 2001. Single-neuron responses to emotional visual stimuli recorded in human ventral prefrontal cortex. Nat Neurosci 4:15–16.

Klausberger T, Magill PJ, Marton LF, Roberts JD, Cobden PM, Buzsaki G, Samogyi P. 2003. Brain-state and cell-type-specific firing of hippocampal interneurons in vivo. Nature 421:844–848.

Kreiman G, Koch C, Fried I. 2000. Imagery neurons in the human brain. Nature 16:357–361.

MacQueen JB. 1967. Some methods for classification and analysis of multivariate observations. In Proceedings of 5th Berkeley Symposium on Mathematical Statistics and Probability. Berkeley: University of California Press. pp 281–297.

Niedermeyer E. 1999. The normal EEG of the waking adult. In: Niedermeyer E, Lopes da Silva F, eds. Electroencephalography: basic principles, clinical applications, and related fields, ed. 4. Philadelphia: Lippincott, Williams & Wilkins. p. 173–174.

Nitz D, McNaughton B. 2004. Differential modulation of CA1 and dentate gyrus interneurons during exploration of novel environments. J Neurophysiol 91:863–872.

Ojemann GA, Schoenfield-McNeill J, Corina D. 2004. Different neurons in different regions of human temporal lobe distinguish correct from incorrect identification or memory. Neuropsychologia 42:1383–1393.

Quiroga RQ, Nadasdy Z, Ben-Shaul Y. 2004. Unsupervised spike detection and sorting with wavelets and superparamagnetic clustering. Neural Comput 16:1661–1687.

Quiroga RQ, Reddy L, Kreiman G, Koch C, Fried I. 2005. Invariant visual representation by single neurons in the human brain. Nature 435:1102–1107.

Ranck JB Jr. 1973. Studies on single neurons in dorsal hippocampal formation and septum in unrestrained rats. I. Behavioral correlates and firing repertoires. Exp Neurol 41:461–531.

Rechtschaffen A, Kales A. 1968. A Manual of Standardized Terminology: Techniques and Storing Systems for Sleep Stages of Human Subjects. Washington, DC: US Government Printing Office.

Rosenow F, Luders LH. 2001. Presurgical evaluation of epilepsy. Brain 124:1683–1700.

Staba RJ, Wilson CL, Bragin A, Fried I, Engel J Jr. 2002a. Sleep states differentiate single neuron activity recorded from human epileptic hippocampus, entorhinal cortex, and subiculum. J Neurosci 22:5694–5704.

Staba RJ, Wilson CL, Fried I, Engel J Jr. 2002b. Single neuron burst firing in the human hippocampus during sleep. Hippocampus 12: 724–734.

Viskontas IV, Knowlton BJ, Steinmetz PN, Fried I. 2006. Differences in mnemonic processing by neurons in the human hippocampus and parahippocampal region. J Cogn Neurosci 18:1654–1662.

Ylinen A, Bragin A, Nadasdy Z, Jando G, Szabo I, Sik A, Buzsaki G. 1995. Sharp wave-associated high-frequency oscillation (200 Hz) in the intact hippocampus: Network and intracellular mechanisms J Neurosci 15:30–46.